Figure 2. Amniotic bistratified neutrophil infiltration in placenta with CAM. *A, C–F,* Amniotic bistratified pattern in Blanc III CAM placenta colonized with *Ureaplasma* spp. *B,* Blanc III CAM placenta colonized with GBS. *A–C,* Mayer's Hematoxylin and eosin (H&E) stain. *D,* Myeloperoxidase. *E,* CD45. *F,* CD68. Arrows indicate infiltrated leukocytes.
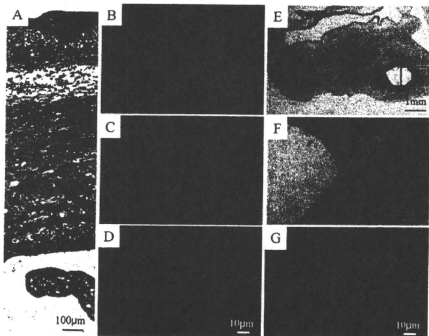

Figure 4. Distribution of *Ureaplasma* spp. and its receptor sulfoglycolipid in placenta. *A,* H&E stain. *B,* PCR for the detection of *Ureaplasma* DNA. (*Upper column*) The *Ureaplasma ureB* gene is detected in genomic DNA from chorioamnion (*lane 1*) but not in villi and decidua (*lanes 2* and *3,* respectively). PC, positive control (full *Ureaplasma* spp. genome). NC, negative control (distilled water). (*Lower column*) The human *Glut1* gene is detected in genomic DNA from chorioamnion, villi, and decidua (*lanes 1, 2* and *3,* respectively). PC, positive control (full human genome). NC, negative control (distilled water). *C, D, Ureaplasma* UreD is detected in the amnion where maternal neutrophils had infiltrated. *E,* Sulfoglycolipid is mainly distributed in the amnion in normal term placenta.

Figure 3. X(red)/Y(green) FISH analysis. (*A*) H&E stain around the membrane. X/Y FISH of (*B*) amnion, (*C*) subchorionic space, and (*D*) villi. (*E*) H&E stain of umbilical cord. (*F*) Higher magnification of umbilical vein and infiltrated cells. (*G*) X/Y FISH of infiltrated cells. One green and one red signal indicate XY karyotype (male, fetus-derived cells) and two red signals indicate XX karyotype (female, maternal-derived cells). DAPI II was used as a counterstain.

the specific neutrophils infiltration of amniotic bistratified pattern, 13 placentas were colonized with *Ureaplasma* spp. solely, five placentas with both *Ureaplasma* spp. and other microorganisms (*Escherichia coli, Pseudomonas fluorescens, Enterobacter cloacae, Candida glabrata, Streptococcus mitis,* or *Clostridium* spp.), and two placentas without any microorganisms (Table 2). None of the placentas, which were nega-
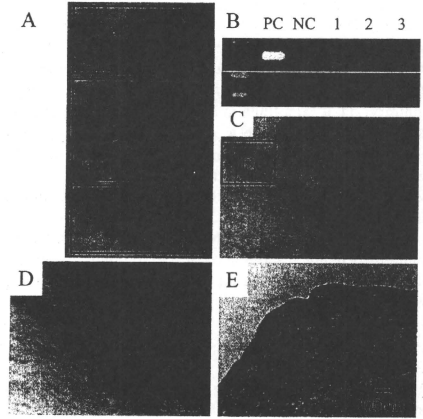
tive for *Ureaplasma* spp. and positive for other microorganisms showed this amniotic bistratified placental pattern.

Specific placental features of intrauterine **Ureaplasma** *infection.* To determine the characteristics of the bistratified infiltrated cells in the amnion and subchorionic space, we analyzed *Ureaplasma*-positive Blanc III CAM placentas and GBS-positive (control) placentas by immunohistochemical staining. Most of the bistratified infiltrated cells in *Ureaplasma*-positive placentas were myeloperoxidase-positive neutrophils, indicating acute inflammation, whereas immunohistochemical staining of CD45 and CD68 were negative (Fig. 2C–F). Control CAM placentas with GBS infection also showed acute inflammation (data not shown).

Next, we analyzed the origin of the migrated neutrophils showing bistratified patterning around the *Ureaplasma*-positive placental membrane (Fig. 3A). Unexpectedly, infiltrated inflammatory cells in the amnion and the subchorionic space showed only two red signals (XX genotype), indicating maternally derived cells (Fig. 3B and C). On the other hand, trophoblasts in the villi and inflammatory cells migrating through the wall of the umbilical vessels (Fig. 3E and F) showed one red and one green signals (fetal XY genotype), as expected (Fig. 3D and G).

To explain these maternal immunologic responses, we further analyzed the localization of the microorganism's DNA in the *Ureaplasma*-positive placenta. PCR amplification of the

Ureaplasma-specific *ureB* gene was detected only in purified genomic DNA from the chorioamnion (Fig. 4*A, B-1*) and not detected in villi (Fig. 4*A, B-2*) or decidua (Fig. 4*A, B-3*) in the paraffin-embedded sections that showed bistratified infiltration of neutrophils (Fig. 4*B, upper column*). On the contrary, PCR amplification of human *Glut1* gene was detected in genomic DNA obtained from chorioamnion, villi, and decidua (Fig. 4*B, lower column*). By immunohistochemical staining with anti-*Ureaplasma* UreD antibody, which was a polyclonal antibody against the *Ureaplasma* urease, positive signals were detected in the amnion where maternal neutrophils had infiltrated (Fig. 4*C* and *D*). Immunohistochemical staining of sulfoglycolipid, the receptor of *Ureaplasma* spp., showed that it was mainly distributed in the amnion in normal term placenta (Fig. 4*E*).

DISCUSSION

Infectious and inflammatory processes in the uterus during pregnancy remain a major cause of preterm delivery and subsequent complications in newborn infants. Pathologic CAM is frequently associated with preterm delivery. The most common microbes isolated from the amniotic cavity of women with preterm labor are *Ureaplasma* spp. and *Mycoplasma hominis* (19). Studies based on the isolation of *Ureaplasma* spp. from the placenta uniformly showed a significant association with CAM (9,10). The stimulatory effect of *Ureaplasma* spp. on cytokine release, such as tumor necrosis factor-α, IL-8, and IL-6, has been confirmed *in vitro* (20–22). Multiple-banded antigen and other lipoproteins from *Ureaplasma* spp. were found to activate nuclear factor kappaB through Toll-like receptor (TLR) 1, TLR2, and TLR6 and induce tumor necrosis factor-α in mouse peritoneal macrophages (23), indicating that not only viable *Ureaplasma* spp. but its lipoproteins cause an excessive immune response *in utero*. Umbilical vasculitis and chorionic plate inflammation might be caused by these antigenic components from local infection. To confirm the association of *Ureaplasma* spp. with CAM, we conducted *Ureaplasma* spp. cultivation as a prospective cohort study of 151 preterm placentas. Furthermore, immunohistochemical, PCR, and FISH analyses were performed in the infected placentas to confirm the microbial localizations.

We examined the incidence of *Ureaplasma* spp. colonization in the placenta by using the culture method. Studies involving various clinical specimens have shown PCR to be more sensitive than conventional culture methods (24–26). However, given the high sensitivity of PCR, a false positive result for a particular organism is more likely to occur than when culture methods are used, principally because of inter-sample contamination. Furthermore, PCR detects nonviable organisms as well as viable organisms, and does not enable further analysis using isolated microorganisms. On the other hand, culture for detection of *Ureaplasma* spp. is expensive and requires specialized media and expertise that are not widely available. We therefore established a culture method for the detection of *Ureaplasma* spp. by modification of the method of Shepard and Lunceford (27) Shepard and Combs

(27,28), which uses materials that are all commercially available and easily prepared just before use.

The relation between infection and preterm delivery is not consistent throughout gestation. Infection is rare in late preterm delivery but is present in most cases in which birth occurs at <30 wk (29,30). Previous evidence suggests that intrauterine infection may occur early in pregnancy. For example, *Ureaplasma* spp. has been detected in some samples of amniotic fluid obtained in routine chromosomal analysis at 15–18 wk of gestation. In most of these women, delivery was around 24 wk (31–33). Meanwhile, Perni *et al.* (34) reported that in 179 asymptomatic women who received amniocentesis at midtrimester, all women with preterm PROM (5/5) tested positive for either *Ureaplasma* spp. or *Mycoplasma hominis* as opposed to none of the women (0/5) with spontaneous preterm birth. In this study, we showed that the incidence of *Ureaplasma* spp. colonization in preterm placentas was statistically higher than that in term placentas ($p < 0.05$) and that the incidence during the second trimester was higher than that during early in the third trimester ($p = 0.05$). We suggest that *Ureaplasma* infection-related CAM might be the leading cause of preterm delivery during the second trimester. One possible explanation for these gestational age-related changes in the cause of preterm delivery is that the intrauterine immune system during the second trimester might be susceptible to weakly pathogenic microorganisms such as *Ureaplasma* spp., and the hormonal immune response or cytokine production necessary to initiate labor is easily activated. In our study, the culture positive for other microorganism (Table 2) was lower (13/151; 8.6%) than those in previous reports (35,36). This discrepancy might be caused by 1) the treatment for inflammation and/or infection by bacteriocidal agents, which reduced the colonization in placentas, and 2) the samples, which we used was the placental surface swab but not by the homogenized tissues.

Although the association between *Ureaplasma* spp. colonization and CAM has already been identified, details of placental features remain unclear. We therefore examined in detail all placentas delivered at <32 wk of gestation and investigated the presence of features specific to *Ureaplasma* spp. colonization. In the CAM placentas, polymorphonuclear leukocytes first accumulate in the intervillous space immediately below the chorionic plate, which forms the roof of this space. The inflammatory cells in the roof of the intervillous space later extend upward into the chorionic plate and reach the amnion. At this stage, the inflammatory cellular response is purely maternal in origin, the leukocytes being derived from maternal blood in the intervillous space (15). According to this migration process, we can simply imagine that this accumulation is composed of one layer of inflammatory cells extending toward the amniotic cavity. However, we found a characteristic pathologic feature named the amniotic bistratified pattern in which leukocytes did not infiltrate in one layer but in two layers. This pathologic pattern was significantly more frequent in placentas colonized with *Ureaplasma* spp. than that in others. Therefore, this amniotic bistratified pattern might be a specific placental feature of intrauterine *Ureaplasma* infection.

To explain how this infiltration pattern develops, we first hypothesized that inflammatory cells in the subchorionic space are derived from maternal sources, but those in the amnion are derived from fetal sources. However, we showed that neutrophils in both the subchorionic space and amnion were maternal cells. On the contrary, infiltrated neutrophils in the umbilical vein were of fetal origin (Fig. 3D and G). Earlier findings might be due to the differences in production and response between maternal and fetal neutrophils. Immature newborn infants frequently become neutropenic (37) in their response to bacterial sepsis. However, adults develop a sustained neutrophil leukocytosis by releasing preformed neutrophils from the marrow storage pool into circulation and increasing proliferation by recruiting a great number of committed granulocyte progenitors into the cell cycle. Furthermore, the most consistently observed functional abnormality of neonatal neutrophils is reduced chemotaxis. In most assays, neutrophils from newborn infants migrate at about half the speed of adult cells (38). Neonatal neutrophils display less interaction with endothelial monolayers in conditions of flow than adult cells. Rolling adhesion is diminished, and fewer cells attach to activated endothelium and migrate to the subendothelial tissue (39). These reports suggest that maternal neutrophils react predominantly at the fetomaternal interface; on the contrary, fetal neutrophils possess the immunologic reaction at least in the fetal side.

Next, we hypothesized that the development of this pattern might be involved in the distribution of genomic DNA and protein from *Ureaplasma* spp. as well as its receptor sulfoglycolipid in the placenta. There are no previous reports of their distribution, but we demonstrated that the urease structural gene and protein of *Ureaplasma* spp. were distributed in the amnion where maternal neutrophils accumulated and that their receptor sulfoglycolipid was also present in the amnion. Therefore, we suggest that this characteristic pattern of maternal neutrophil infiltration in the amnion might be associated with the distribution of *Ureaplasma* spp. and its receptor in the placenta.

In conclusion, our study indicates the following: 1) ~40–50% of preterm placentas delivered at <32 wk of gestation are culture positive for *Ureaplasma* spp.; 2) placentas colonized with *Ureaplasma* spp. show CAM significantly more frequently than others; 3) positivity of cultures for *Ureaplasma* spp. is an independent risk factor for CAM; 4) positivity of cultures for *Ureaplasma* spp. is also associated with the severity of CAM; and 5) the amniotic bistratified pattern in CAM might be a specific placental feature for intrauterine *Ureaplasma* infection.

REFERENCES

1. Waites KB, Schelonka RL, Xiao L, Grigsby PL, Novy MJ 2009 Congenital and opportunistic infections: *Ureaplasma* species and *Mycoplasma hominis*. Semin Fetal Neonatal Med 14:190–199

2. Taylor-Robinson D, McCormack WM 1980 The genital mycoplasmas. N Engl J Med 302:1003–1010

3. Cassell GH, Waites KB, Watson HL, Crouse DT, Harasawa R 1993 *Ureaplasma urealyticum* intrauterine infection: role in prematurity and disease in newborns. Clin Microbiol Rev 6:69–87

4. Goldenberg RL 2002 The management of premature labor. Obstet Gynecol 100:1020–1037

5. Wood NS, Marlow N, Costeloe K, Gibson AT, Wilkinson AR 2000 Neurologic and developmental disability after extremely preterm birth. EPICure Study Group. N Engl J Med 343:378–384

6. Goldenberg RL, Rouse DJ 1998 Prevention of preterm birth. N Engl J Med 339:313–320

7. Shurin PA, Alpert S, Bernard Rosner BA, Driscoll SG, Lee YH 1975 Chorioamnionitis and colonization of the newborn infant with genital mycoplasmas. N Engl J Med 293:5–8

8. Hillier SL, Martius J, Krohn M, Kiviat N, Holmes KK, Eschenbach DA 1988 A case-control study of chorioamnionic infection and histologic chorioamnionitis in prematurity. N Engl J Med 319:972–978

9. Kundsin RB, Driscoll SG, Monson RR, Yeh C, Biano SA, Cochran WD 1984 Association of *Ureaplasma urealyticum* in the placenta with perinatal morbidity and mortality. N Engl J Med 310:941–945

10. Embree JE, Krause VW, Embil JA, MacDonald S 1980 Placental infection with *Mycoplasma hominis* and *Ureaplasma urealyticum*: clinical correlation. Obstet Gynecol 56:475–481

11. Honma Y, Yada Y, Takahashi N, Momoi MY, Nakamura Y 2007 Certain type of chronic lung disease of newborns is associated with *Ureaplasma urealyticum* infection in utero. Pediatr Int 49:479–484

12. Naessens A, Foulon W, Cammu H, Goossens A, Lauwers S 1987 Epidemiology and pathogenesis of *Ureaplasma urealyticum* in spontaneous abortion and early preterm labor. Acta Obstet Gynecol Scand 66:513–516

13. Revesz T, Greaves M 1975 Ligand-induced redistribution of lymphocyte membrane ganglioside GM1. Nature 257:103–106

14. Lingwood CA, Quinn PA, Wilansky S, Nutikka A, Ruhnke HL, Miller RB 1990 Common sulfoglycolipid receptor for mycoplasmas involved in animal and human infertility. Biol Reprod 43:694–697

15. Fox H, Sebire NJ eds 2007 Pathology of the Placenta. Saunders Elsevier, Philadelphia

16. Blanc WA 1981 Pathology of the placenta, membranes, and umbilical cord in bacterial, fungal and viral infections in man. Monogr Pathol 67–132

17. Kong F, Zhu X, Wang W, Zhou X, Gordon S, Gilbert GL 1999 Comparative analysis and serovar-specific identification of multiple-banded antigen genes of *Ureaplasma urealyticum* biovar 1. J Clin Microbiol 37:538–543

18. Cheng X, Zhang Y, Kotani N, Watanabe T, Lee S, Wang X, Kawashima I, Tai T, Taniguchi N, Honke K 2005 Production of a recombinant single-chain variable-fragment (scFv) antibody against sulfoglycolipid. J Biochem 137:415–421

19. Romero R, Mazor M 1988 Infection and preterm labor. Clin Obstet Gynecol 31:553–584

20. Manimtim WM, Hasday JD, Hester L, Fairchild KD, Lovchik JC, Viscardi RM 2001 *Ureaplasma urealyticum* modulates endotoxin-induced cytokine release by human monocytes derived from preterm and term newborns and adults. Infect Immun 69:3906–3915

21. Li YH, Brauner A, Jonsson B, van der Ploeg I, Soder O, Holst M, Jensen JS, Lagercrantz H, Tullus K 2000 *Ureaplasma urealyticum*-induced production of proinflammatory cytokines by macrophages. Pediatr Res 48:114–119

22. Viscardi RM, Hasday JD 2009 Role of *Ureaplasma* species in neonatal chronic lung disease: epidemiologic and experimental evidence. Pediatr Res 65:84R–90R

23. Shimizu T, Kida Y, Kuwano K 2008 *Ureaplasma parvum* lipoproteins, including MB antigen, activate NF-kappaB through TLR1, TLR2 and TLR6. Microbiology 154:1318–1325

24. Teng K, Li M, Yu W, Li H, Shen D, Liu D 1994 Comparison of PCR with culture for detection of *Ureaplasma urealyticum* in clinical samples from patients with urogenital infections. J Clin Microbiol 32:2232–2234

25. Abele-Horn M, Wolff C, Dressel P, Zimmermann A, Vahlensieck W, Pfaff F, Ruckdeschel G 1996 Polymerase chain reaction versus culture for detection of *Ureaplasma urealyticum* and *Mycoplasma hominis* in the urogenital tract of adults and the respiratory tract of newborns. Eur J Clin Microbiol Infect Dis 15:595–598

26. Cunliffe NA, Fergusson S, Davidson F, Lyon A, Ross PW 1996 Comparison of culture with the polymerase chain reaction for detection of *Ureaplasma urealyticum* in endotracheal aspirates of preterm infants. J Med Microbiol 45:27–30

27. Shepard MC, Lunceford CD 1978 Serological typing of *Ureaplasma urealyticum* isolates from urethritis patients by an agar growth inhibition method. J Clin Microbiol 8:566–574

28. Shepard MC, Combs RS 1979 Enhancement of *Ureaplasma urealyticum* growth on a differential agar medium (A7B) by a polyamine, putrescine. J Clin Microbiol 10:931–933

29. Watts DH, Krohn MA, Hillier SL, Eschenbach DA 1992 The association of occult amniotic fluid infection with gestational age and neonatal outcome among women in preterm labor. Obstet Gynecol 79:351–357

30. Chellam VG, Rushton DI 1985 Chorioamnionitis and funiculitis in the placentas of 200 births weighing less than 2.5 kg. Br J Obstet Gynaecol 92:808–814

31. Gray DJ, Robinson HB, Malone J, Thomson RB Jr 1992 Adverse outcome in pregnancy following amniotic fluid isolation of *Ureaplasma urealyticum*. Prenat Diagn 12:111–117

32. Horowitz S, Mazor M, Romero R, Horowitz J, Glezerman M 1995 Infection of the amniotic cavity with *Ureaplasma urealyticum* in the midtrimester of pregnancy. J Reprod Med 40:375–379

33. Nguyen DP, Gerber S, Hohlfeld P, Sandrine G, Witkin SS 2004 *Mycoplasma hominis* in mid-trimester amniotic fluid: relation to pregnancy outcome. J Perinat Med 32:323–326

34. Perni SC, Vardhana S, Korneeva I, Tuttle SL, Paraskevas LR, Chasen ST, Kalish RB, Witkin SS 2004 *Mycoplasma hominis* and *Ureaplasma urealyticum* in midtrimester amniotic fluid: association with amniotic fluid cytokine levels and pregnancy outcome. Am J Obstet Gynecol 191:1382–1386

35. Onderdonk AB, Delaney ML, DuBois AM, Allred EN, Leviton A; Extremely Low Gestational Age Newborns (ELGAN) Study Investigators 2008 Detection of bacteria in placental tissues obtained from extremely low gestational age neonates. Am J Obstet Gynecol 198:110.e1–110.e7

36. Svensson L, Ingemarsson I, Mårdh PA 1986 Chorioamnionitis and the isolation of microorganisms from the placenta. Obstet Gynecol 67:403–409

37. Christensen RD 1989 Neutrophil kinetics in the fetus and neonate. Am J Pediatr Hematol Oncol 11:215–223

38. Wolach B, Sonnenschein D, Gavrieli R, Chomsky O, Pomeranz A, Yuli I 1998 Neonatal neutrophil inflammatory responses: parallel studies of light scattering, cell polarization, chemotaxis, superoxide release, and bactericidal activity. Am J Hematol 58:8–15

39. Anderson DC, Abbassi O, Kishimoto TK, Koenig JM, McIntire LV, Smith CW 1991 Diminished lectin-, epidermal growth factor-, compliment binding domain-cell adhesion molecule-1 on neonatal neutrophils underlies their impaired CD18-independent adhesion to endothelial cells in vitro. J Immunol 146:3372–3379

Expression patterns of connective tissue growth factor and of TGF-β isoforms during glomerular injury recapitulate glomerulogenesis

Yasuhiko Ito,[1,2] Roel Goldschmeding,[3] Hirotake Kasuga,[4] Nike Claessen,[1] Masahiro Nakayama,[5] Yukio Yuzawa,[2] Akiho Sawai,[2] Seiichi Matsuo,[2] Jan J. Weening,[1] and Jan Aten[1]

[1]Department of Pathology, Academic Medical Center, University of Amsterdam, Amsterdam, The Netherlands; [2]Department of Nephrology, Nagoya University, Nagoya, Japan; [3]Department of Pathology, University Medical Centre Utrecht, Utrecht, The Netherlands; [4]Department of Internal Medicine, Nagoya Kyoritsu Hospital, Nagoya; and [5]Department of Clinical Laboratory Medicine and Anatomic Pathology, Osaka Medical Center and Research Institute for Maternal and Child Health, Osaka, Japan

Ito Y, Goldschmeding R, Kasuga H, Claessen N, Nakayama M, Yuzawa Y, Sawai A, Matsuo S, Weening JJ, Aten J. Expression patterns of connective tissue growth factor and of TGF-β isoforms during glomerular injury recapitulate glomerulogenesis. Am J Physiol Renal Physiol 299: F545–F558, 2010. First published June 24, 2010; doi:10.1152/ajprenal.00120.2009.—Transforming growth factor (TGF)-β1, -β2, and -β3 are involved in control of wound repair and development of fibrosis. Connective tissue growth factor (CTGF) expression is stimulated by all TGF-β isoforms and is abundant in glomerulosclerosis and other fibrotic disorders. CTGF is hypothesized to mediate profibrotic effects of TGF-β1 or to facilitate interaction of TGF-β1 with its receptor, but its interactions with TGF-β isoforms in nonpathological conditions are unexplored so far. Tissue repair and remodeling may recapitulate gene transcription at play in organogenesis. To further delineate the relationship between CTGF and TGF-β, we compared expression patterns of CTGF and TGF-β isoforms in rat and human glomerulogenesis and in various human glomerulopathies. CTGF mRNA was present in the immediate precursors of glomerular visceral and parietal epithelial cells in the comma- and S-shaped stages, but not in earlier stages of nephron development. During the capillary loop and maturing glomerular stages and simultaneous with the presence of TGF-β1, -β2, and -β3 protein, CTGF mRNA expression was maximal and present only in differentiating glomerular epithelial cells. CTGF protein was also present on precursors of mesangium and glomerular endothelium, suggesting possible paracrine interaction. Concomitant with the presence of TGF-β2 and -β3 protein, and in the absence of TGF-β1, CTGF mRNA and protein expression was restricted to podocytes in normal adult glomeruli. However, TGF-β1 and CTGF were again coexpressed, often with TGF-β2 and -β3, in particular in podocytes in proliferative glomerulonephritis and also in mesangial cells in diabetic nephropathy and IgA nephropathy (IgA NP). Coordinated expression of TGF-β isoforms and of CTGF may be involved in normal glomerulogenesis and possibly in maintenance of glomerular structure and function at adult age. Prolonged overexpression of TGF-β1 and CTGF is associated with development of severe glomerulonephritis and glomerulosclerosis.

CCN2; development; glomerulosclerosis; podocyte

CONNECTIVE TISSUE GROWTH FACTOR (CTGF or CCN2) is a member of the CCN family of structurally related proteins (11, 14, 21). The CCN proteins contain an NH_2-terminal secretory signal peptide and four structural domains: an insulin-like growth factor binding domain (*domain 1*); a chordin-like, cysteine-rich domain with similarity to von Willebrand factor

type C domain (*domain 2*), which is connected via a protease-sensitive hinge region to a thrombospondin type I repeat (*domain 3*); and finally a COOH-terminal cystine knot (*domain 4*) (1, 11). CCN proteins are involved in regulation of essential cell functions such as adhesion, migration, mitogenesis, differentiation, and survival (13, 29). As such, CCN family members have been implicated among others in control of wound repair, development of fibrosis, and tumorigenesis (20, 30, 44). CTGF, in particular, has been reported to be overexpressed in fibrosis of diverse organs (22, 34, 40, 42). Our laboratory demonstrated that CTGF mRNA is strongly upregulated in human fibrosis and in rat experimental proliferative glomerulonephritis (23, 24).

Transforming growth factor (TGF)-β is a key component in control of wound repair and in development of fibrosis (7, 10). CTGF mRNA expression was observed to be associated with differential expression of the three closely related isoforms of TGF-β in the course of the anti-Thy-1.1 glomerulonephritis model (24). All three TGF-β isoforms are equally able to induce upregulation of CTGF mRNA in both cultured mesangial cells and glomerular visceral epithelial cells (GVECs) (24). In vitro effects of TGF-β1 on matrix synthesis by fibroblasts and mesangial cells do, at least partially, require the presence of CTGF (9, 30, 67). These findings suggest that CTGF may be involved in tissue repair in response to glomerular injury, possibly downstream of TGF-β. Tissue repair may recapitulate developmental programs at play in organogenesis, and comparison of these processes may yield insight in the nature of common regulatory factors. In development of the kidney in mammals, the ureteric bud is induced by the metanephric blastema to develop from the mesonephric duct. Growth of the ureteric duct comprises both elongation of the duct and (asymmetric) branching. In turn, the metanephric blastema is induced by the invading ureter branch tips to undergo nephrogenesis involving mesenchymal cell condensation and transition into polarized epithelium forming a vesicle. The vesicle undergoes patterning to form subsequently comma-shaped and S-shaped bodies. Capillary sprouts, as well as vasculogenic precursors of endothelial cells, are recruited into the cleft that is formed by the proximal curvature of the S-shaped body. The proximal and distal parts of the S-shaped body differentiate into the glomerular epithelium and into the proximal and distal tubular epithelium, respectively.

Glomerulogenesis proceeds through the capillary loop stage and the maturing stage to the adult stage, during which mesangial progenitor cells migrate into the glomerulus, the glo-

tion of the purified insert was performed using SP6 or T7 RNA polymerases and digoxigenin (DIG)-conjugated UTP (Roche, Almere, The Netherlands) to produce DIG-labeled sense or antisense riboprobes. The specificity of the DIG-labeled CTGF antisense riboprobe was examined by Northern blotting of total RNA, isolated from kidneys of 9-days-old rats, and from established lines of glomerular visceral epithelial cells (GVEC) derived from rat, mouse, and human kidneys (28, 35, 46, 58).

ISH and immunohistology double staining. Six-micrometer-thick sections of formalin-fixed, paraffin-embedded tissue were dewaxed, rehydrated, incubated with 20 μg/ml proteinase K (Life Technologies, Breda, The Netherlands) in PBS at 37°C for 15 min, treated with 0.2% glycine in PBS, washed in PBS, and postfixed with 2% paraformaldehyde and 0.1% glutaraldehyde in PBS for 20 min. After prehybridization for 1 h at 70°C, hybridization with 250 ng/ml CTGF DIG-labeled riboprobe in hybridization buffer [50% formamide, 5× standard sodium citrate (SSC), 1% blocking reagent (Roche), 5 mM EDTA, 0.1% Tween-20, 0.1% CHAPS, 0.1 mg/ml heparin, 1 mg/ml yeast tRNA] was performed at 70°C for 16 h. Slides were briefly rinsed in 2× SSC and subsequently washed twice in 2× SSC containing 50% formamide, for 15 min each at 65°C, followed by washing in PBS, 0.1% Tween-20 (PBS/T). After nonspecific binding sites were blocked by 2% blocking reagent in PBS/T, sections were incubated for 2 h with alkaline phosphatase-conjugated sheep anti-DIG antibodies (Roche), diluted to 1:1,500 in blocking buffer. After being washed in PBS/T and in 0.1 M Tris, pH 9.5, 0.1 M NaCl, 0.05 M MgCl₂, and 0.05% Tween-20 (NTM/T), alkaline phosphatase activity was detected with nitroblue tetrazolium chloride and 5-bromo-4-chloro-3-indolylphosphate, toluidine salt ready-made solution (Roche), diluted to 1:50 in NTM/T. After overnight incubation at 20°C, sections were rinsed with distilled water. Subsequently, immunohistochemistry was performed for collagen type IV to provide a counterstain that does not interfere with the cellularly localized ISH signals. Briefly, endogenous peroxidase activity was inactivated, nonspecific protein binding sites were blocked with 10% normal goat serum in PBS, and sections were incubated for 1 h with rabbit anti-collagen type IV (Euro-Diagnostica, Arnhem, The Netherlands), diluted to 1:100 in PBS. After washing, sections were incubated with poly-horseradish peroxidase (HRP) goat anti-rabbit IgG (Powervision, Immunovision Technologies) for 10 min, followed by washing in PBS. HRP activity was detected using 3,3'-diaminobenzidine and hydrogen peroxide. Sections were dehydrated and mounted with Pertex.

Polyclonal and monoclonal CTGF-specific antibodies. Polyclonal antibodies were raised in rabbit against an 11-amino acid peptide, i.e., CEADLEENIKK, corresponding to amino acid residues 242–252 of human CTGF (GenBank accession number P29279), 241–251 of mouse CTGF (GenBank P29268), and 240–250 of rat CTGF (GenBank AAD39132). The CEADLEENIKK sequence is located in between domain 3 and domain 4 of CTGF and does not occur in other members of the CCN family of structurally related proteins. Rabbit IgG antibodies were affinity purified to the linear peptide. A human IgG₁ monoclonal antibody (FG-3019) and a mouse IgG₁ monoclonal antibody (FG-3145) that bind distinct epitopes in domain 2 of CTGF (61) were kindly supplied by FibroGen (FibroGen, South San Francisco, CA). FG-3019 was produced in Medarex mice (Medarex, Princeton, NJ) by immunization with recombinant human CTGF. The recombinant human CTGF was produced in a baculovirus expression system (FibroGen). The specificity of the antibodies was analyzed by Western blotting of cell lysates of murine NIH/3T3 or rat NRK-49F fibroblasts (obtained from ATCC, Manassas, VA) that were cultured for 24 h, with or without recombinant human TGF-β₁ (R&D Systems). In addition, ELISA to recombinant fragments of CTGF and to full-length recombinant CTGF was performed for the rabbit anti-CEADLEENIKK.

Immunohistochemistry. For immunohistochemistry on rat kidney, 4-μm-thick sections were cut from formalin-fixed, paraffin-embedded

tissue. After dewaxing and rehydration of the sections, the slides were incubated with protease XXIV (Sigma) at 4 U/ml in 0.1 M phosphate buffer, pH 7.8, for 3 min at 37°C. After washing, the slides were heated in 0.04 M citrate, 0.12 M phosphate, pH 5.8, for 3 min at 100°C by microwave. Subsequently, the slides were washed in PBS, and endogenous peroxidase activity was blocked by incubation in 1% H₂O₂ in PBS for 20 min. After washing and blocking of nonspecific protein binding sites by incubation in normal goat serum (Dako, Glostrup, Denmark), the sections were incubated with FG-3019 anti-CTGF, at 1 μg/ml in PBS/5% BSA for 16 h at 4°C. After washing, sections were subsequently incubated with rabbit anti-human IgG (diluted to 1:5,000 in PBS/10% normal rat serum; Dako), washed, and incubated with undiluted poly-HRP goat anti-rabbit IgG (PowerVision; ImmunoVision Technologies, Springdale, AR). HRP activity was detected using 3,3'-diaminobenzidine as substrate. Sections were counterstained with methyl-green and were mounted with pertex.

For immunohistochemistry on human kidney, 4-μm-thick sections of formalin-fixed, paraffin-embedded tissues were deparaffinated and rehydrated. The sections were incubated in 0.3% H₂O₂ in methanol to block endogenous peroxidase activity. Antigen retrieval was performed by heating in 10 mM Tris·HCl and 1 mM EDTA, pH 9.0, for 10 min at 100°C. After washing, the sections were incubated with FG-3145 anti-human CTGF at 1 μg/ml in Antibody Diluent (ImmunoLogic, Klinipath, Duiven, The Netherlands) for 16 h at 4°C, washed, and incubated with poly-HRP goat anti-mouse IgG (Bright-Vision, ImmunoLogic). HRP activity was detected using 3,3'-diaminobenzidine as substrate. Sections were counterstained with methyl-green and were mounted with pertex.

In addition, immunohistochemistry on human and rat kidneys was performed on cryostat sections. Four-micrometer-thick sections were fixed in methanol for CTGF immunochemistry and in acetone for TGF-β₁, TGF-β₂, and TGF-β₃ immunohistochemistry. Endogenous peroxidase activity was inhibited with 0.1% NaN₃ and 0.3% H₂O₂, and nonspecific protein binding sites were blocked with normal goat serum. The sections were incubated with rabbit polyclonal IgG anti-CEADLEENIKK antibody for 16 h at 4°C. Other sections were incubated with rabbit polyclonal IgG anti-TGF-β₁, anti-TGF-β₂, or anti-TGF-β₃ (Santa Cruz Biotechnology, Santa Cruz, CA) for 4 h at room temperature. The polyclonal anti-TGF-β₁, anti-TGF-β₂, and anti-TGF-β₃ antibodies were raised against peptides that map at or near the carboxy terminal ends, corresponding to amino acid residues 328–353 (GenBank accession number P01137), 352–377 (P08112), and 350–374 (P10600), respectively. The antibodies are expected to bind both the bioactive and the latent conformations of the TGF-β isoforms (36). HRP-labeled polyclonal goat anti-rabbit IgG antibodies (EnVision System, Dako) were applied as secondary reagent. Finally, enzyme activity of HRP was detected using 3,3'-diaminobenzidine tetrahydrochloride liquid system (Dako). Negative controls were performed by preabsorbing the polyclonal anti-CTGF antibodies with the free CEADLEENIKK peptide and by replacing first-step antibodies for species-matched Ig. Mesangial CTGF protein expression was analyzed and semiquantitatively classified into five groups: 0, no staining; 1, weak staining; 2, segmental or diffuse weak staining; 3, diffuse staining; and 4, strong diffuse staining. For each glomerulus, the "mesangial CTGF protein expression score" was assessed, and the average of the score in each patient was calculated.

To compare localization of CTGF and TGF-β isoforms with that of the glomerular cell types in the developing kidney, we performed IHC on consecutive sections for synaptopodin as marker of GVECs (5, 6) using MAb G1D4 (mouse IgG₁; Progen, Heidelberg, Germany), for CD31 as marker of endothelial cells (39) using MAb JC/70A (mouse IgG1; Dako), and for α-smooth muscle actin (α-SMA) as marker of fetal and activated mesangial cells (2, 39) using MAb 1A4 (mouse IgG₂ₐ; Dako). In addition, expression of the EDA-domain-containing "cellular" splice variant of fibronectin (EDA-FN) (12) and expression of collagen type IV were studied, using MAb IST-9 (mouse IgG1; Accurate Chemical & Scientific, Westbury, NY) and rabbit anti-

collagen type IV polyclonal antibody (Chemicon International, Temecula, CA), respectively. Binding of these reagents was detected with HRP-conjugated goat anti-mouse IgG antibodies or HRP-conjugated goat anti-rabbit IgG antibodies (EnVision System, Dako). Negative controls were performed by replacement of the first-step antibody with incubation buffer only or with isotype- and species-matched antibodies. HRP activity was detected using 3,3'-diaminobenzidine tetrahydrochloride liquid system (Dako) or 3-amino-9-ethyl-carbazole (Dako).

Confocal laser scanning microscopy. To examine the localization of CTGF during normal human glomerulogenesis in detail, two-color immunofluorescence histology was performed on methanol-fixed, 4-μm-thick sections that were preincubated with 10% normal goat serum. Sections were incubated with rabbit anti-CEADLEENIKK antibody for 16 h at 4°C, followed by rhodamine-labeled donkey anti-rabbit F(ab')₂ antibodies (Chemicon International) absorbed with normal human serum. Subsequently, monoclonal anti-synaptopodin, anti-α-SMA, or anti-CD31 antibodies were applied for 30 min. Then sections were incubated with fluorescein isothiocyanate (FITC)-conjugated rabbit anti-mouse F(ab')₂ antibodies (Zymed Laboratories, San Francisco, CA), absorbed with normal human serum. After the final wash with Tris-buffered saline, all sections were mounted with medium containing *p*-phenylenediamine. Confocal laser scanning microscopy was performed using a Bio-Rad MRC-1024 scan head (Bio-Rad, Hercules, CA) attached to a microscope E800 (Nikon, Tokyo, Japan), applying double excitation with a 488-nm band-pass filter for FITC emission, and a 568-nm long-pass filter for rhodamine emission. Both images were adjusted to the full dynamic range. Subsequently, FITC- and rhodamine-derived images were corrected for cross talk and merged using the Laser Sharp Acquisition Software (Bio-Rad, Tokyo, Japan) and a look-up table to convert FITC signals to green, rhodamine signals to red, and overlapping areas to yellow.

Statistical analysis. Data of the mesangial CTGF score are not normally distributed and are, therefore, presented as median values and ranges. Statistical analysis was performed using the Kruskal-Wallis test, and groups were compared using Dunn's multiple-comparison test (GraphPad Software, La Jolla, CA).

RESULTS

Characterization of CTGF-specific antisense riboprobe and antibodies. Northern blotting demonstrated binding of the DIG-labeled CTGF antisense riboprobe to a 2.4-kb RNA, which corresponds to the reported size of CTGF mRNA. As expected, more probe was bound to RNA isolated from cell cultures that had been exposed to TGF-β₁, compared with RNA from control cell cultures (Fig. 1A).

Western blot analysis revealed specific binding of both rabbit anti-CEADLEENIKK polyclonal IgG and human FG-3019 to proteins of 38 kDa and 35–36 kDa, corresponding to the size of CTGF under reducing and nonreducing conditions, respectively (Fig. 1B). Both rabbit anti-CEADLEENIKK and FG-3019 did bind recombinant human CTGF in a doublet, possibly due to heterogeneous glycosylation of the recombinant CTGF, which was also detected in the NRK-49F cell lysate with FG-3019. In addition to the full-size protein, 10-kDa proteins were detected by rabbit-anti-CEADLEENIKK in some samples; these proteins may be degradation products of CTGF. Preincubation of rabbit anti-CEADLEENIKK with the peptide that was used as immunogen blocked binding to CTGF; preimmune rabbit serum and normal human serum demonstrated only weak background binding (not shown). ELISA confirmed binding of rabbit anti-CEADLEENIKK to the purified recombinant COOH-terminal fragment of CTGF, containing domains 3 and 4, as well as to full-length recombinant
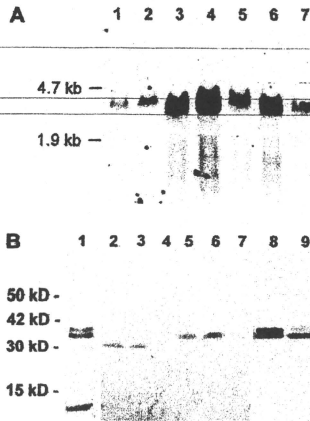

Fig. 1. *A*: Northern blotting using a digoxigenin-labeled antisense riboprobe reveals connective tissue growth factor (CTGF) mRNA in glomerular visceral epithelial cell lines of human (*lanes 1* and *2*), mouse (*lanes 3* and *4*), and rat (*lanes 5* and *6*) origin that were cultured without (*lanes 1, 3,* and *5*) or with transforming growth factor (TGF)-β₁ (5 ng/ml for 24 h; *lanes 2, 4,* and *6*), as well as in rat kidney (*lane 7*). *B*: Western blotting using rabbit anti-CEADLEENIKK shows the presence of CTGF protein in the supernatant of TGF-β₁-stimulated NIH/3T3 cells under both nonreducing (*lanes 2* and *3*) and reducing conditions (*lanes 5* and *6*). CTGF protein is not detected in the supernatant of NIH/3T3 fibroblasts that were cultured without TGF-β₁ (*lanes 4* and *7*). Both rabbit anti-CEADLEENIKK peptide and monoclonal human anti FG-3019 bind recombinant human CTGF in a doublet (*lanes 1* and *8*, respectively), which was also detected in lysate of TGF-β₁-stimulated rat NRK-49F cells using FG-3019 (*lane 9*); samples in *lanes 1, 8,* and *9* were prepared under reducing conditions.

CTGF, and absence of binding to the NH₂-terminal fragment of CTGF, containing domains 1 and 2 (Supplemental Fig. S1; the online version of this article contains supplemental data).

CTGF mRNA and protein expression during glomerulogenesis in the rat. In the first week after birth, all stages of glomerular development can be examined in the rat kidney. ISH with the CTGF antisense riboprobe revealed CTGF mRNA expression in the proximal part of comma- and S-shaped bodies containing the immediate precursors of visceral and parietal glomerular epithelial cells (Fig. 2A, arrowhead and short arrow, respectively). CTGF mRNA expression was highest in later stages of glomerular development, i.e., in the capillary loop stage and the maturing stages (Figs. 2, A, long arrow, and C, respectively), where it is mainly observed in the periphery of the glomeruli, indicating preferential expression by glomerular epithelial cells. Throughout renal development, CTGF mRNA was expressed in the media of arcuate (Fig. 2C, inset) and interlobular arteries and could also be found in endothelial cells of the large venes. Also, in the vessel walls of the afferent arterioles, CTGF mRNA was observed (Fig. 2C). In adult glomeruli, CTGF mRNA expression was detected in podocytes and occasionally in glomerular parietal epithelial cells (Fig. 2E). In all stages of development, tubular epithelial cells of all compartments of the nephron expressed CTGF
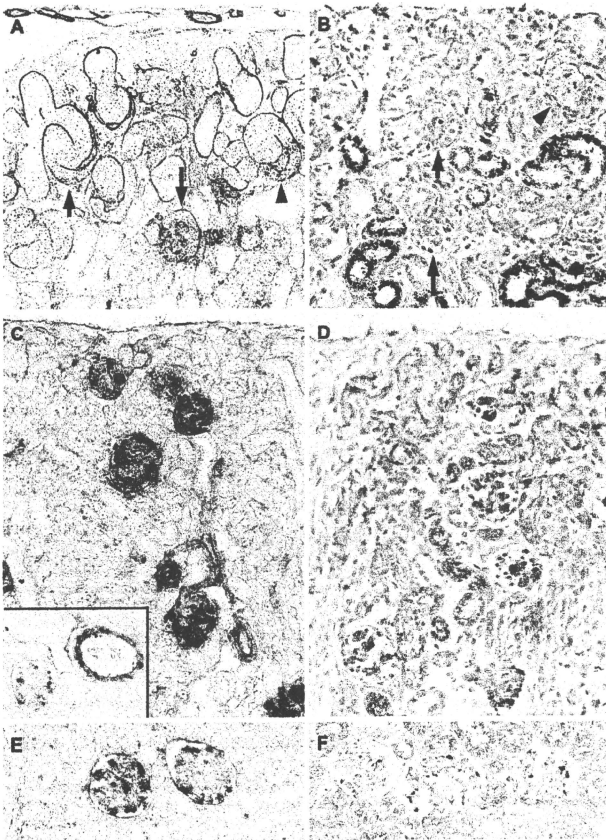
Fig. 2. Expression of CTGF mRNA (*A*, *C*, and *E*; in situ hybridization, blue signal) and CTGF protein (*B*, *D*, and *E*; immunostaining using FG-3019, brown signal) in rat kidneys at ages of 1 day (*A* and *B*), 9 days (*C* and *D*), and 2 mo (*E* and *F*). Counterstains are either type IV collagen immunostaining (*A* and *C*; brown signal) or methyl-green (*B*, *D*, and *E*). Original magnifications: ×200 (*A–F*), or ×400 (*inset* in *C*). CTGF mRNA is detected in comma- and S-shaped bodies (*A*; arrowhead and short arrow, respectively), in the capillary loop stage (*A*; long arrow), in maturing glomerular stages (*C*), and in adult glomeruli (*E*). CTGF mRNA is also present in afferent arterioles (*C*) and in the media of arcuate (*C*, *inset*) and interlobular arteries. CTGF protein is very weakly stained in only some epithelial cells in comma- and S-shaped bodies and in capillary loop stages (*B*; arrowhead, short arrow, and long arrow, respectively). CTGF protein is readily detected in maturing and adult glomeruli (*D* and *F*, respectively). Subsets of tubular epithelial cells stain strongly for CTGF in neonatal kidney (*B*); tubular staining intensity is less in kidneys at *day 9* (*D*).

mRNA at most to a minor extent in a diffuse pattern. As controls, ISH with an oligo(dT) probe yielded positive staining of virtually all cells in the tissue under examination, ISH with a von Willebrand factor antisense probe resulted in staining of only endothelia of the large vessels (not shown). ISH with the control CTGF sense probe did not yield staining (Supplemental Fig. S2).

CTGF protein was very weakly stained using FG-3019 in only some epithelial cells in the comma- and S-shaped bodies (Fig. 2*B*). In glomeruli of the capillary loop stage and in the maturing stage, CTGF protein was detected mostly in the periphery of the glomeruli, suggesting the presence of CTGF in differentiating parietal and visceral epithelial cells (Fig. 2*D*). In adult glomeruli, CTGF protein was frequently present in podocytes (Fig. 2*F*). At *days 1* and *2* after birth, strong staining for CTGF was observed in a subset of tubular epithelial cells (Fig.

2*B*). Staining for CTGF in tubules was less abundant at *days 5* and 9 (Fig. 2*D*). Some faint staining for CTGF was found in large-vessel walls. Epithelial cells in capillary loop and maturing stage glomeruli were also stained with the rabbit anti-CEADLEENIKK antibody, directed against the COOH-terminal part of CTGF, whereas staining of the tubular portion of the nephron was not detected. In contrast, rabbit anti-CEADLEENIKK, but not FG-3019, did bind to structures in association with the developing cortical collecting ducts in the medullary ray area (Supplemental Fig. S3). Incubations with normal human serum instead of FG-3019 on paraffin sections or with preimmune normal rabbit serum instead of rabbit anti-CEADLEENIKK on cryostat sections did not yield any staining, indicating that detection of the primary antibodies by the secondary reagents was specific (Supplemental Fig. S3).

— 202 —

Expression of CTGF mRNA and protein in fetal and control adult human kidney. Kidneys from 15- to 23-wk-old human fetuses typically contain ureteric buds, metanephric blastema, and glomeruli of all stages of development. CTGF mRNA was very weakly detected in comma- and S-shaped glomerular stages (Fig. 3A) and strongly in the early and late capillary loop stages (Figs. 3, A, B, and D) mainly in parietal and visceral epithelial cells. In the subsequent maturing stages (Fig. 3A), CTGF mRNA was predominantly present in the transitional area between parietal and GVECs (Fig. 3A). In control adult glomeruli, CTGF mRNA was detected in some podoyctes (see Fig. 7).

CTGF protein expression was not observed in the renal vesicles and in the S-shaped body stage of the fetal kidneys when using either mouse FG-3145 or rabbit anti-CEADLEENIKK (not shown). In contrast, CTGF was present in the capillary loop-stage glomeruli, as detected with FG-3145 (Fig. 3, C and E) or with rabbit anti-CEADLEENIKK (Figs. 4A, 5, and 6), and to a lesser extent in maturing glomeruli (Figs. 4B, 5, and 6), and also in adult glomeruli (Figs. 4C, 5, and 6) and in distal parts of nephrons (not shown).

In the capillary loop stage, CTGF expression was strongest at the basal part of the GVECs and was also present in a

Fig. 3. Expression of CTGF mRNA (*A, B,* and *D*; in situ hybridization, blue signal; no counterstain) and CTGF protein (*C* and *E*; immunostaining using FG-3145, brown signal; methyl-green counterstain) in glomeruli at the capillary loop stage and at the maturing stage in human fetal kidneys. CTGF mRNA is very weakly detected in comma- and S-shaped bodies (*A*), and strongly in glomerular epithelial cells in capillary loop stages (*A, B,* and *D*). CTGF protein is detected predominantly in visceral epithelial cells and weakly in mesangial and/or endothelial cells in capillary loop-stage glomeruli (*C* and *E*). Bar sizes: 100 μm (*A*), 25 μm (*B–E*).
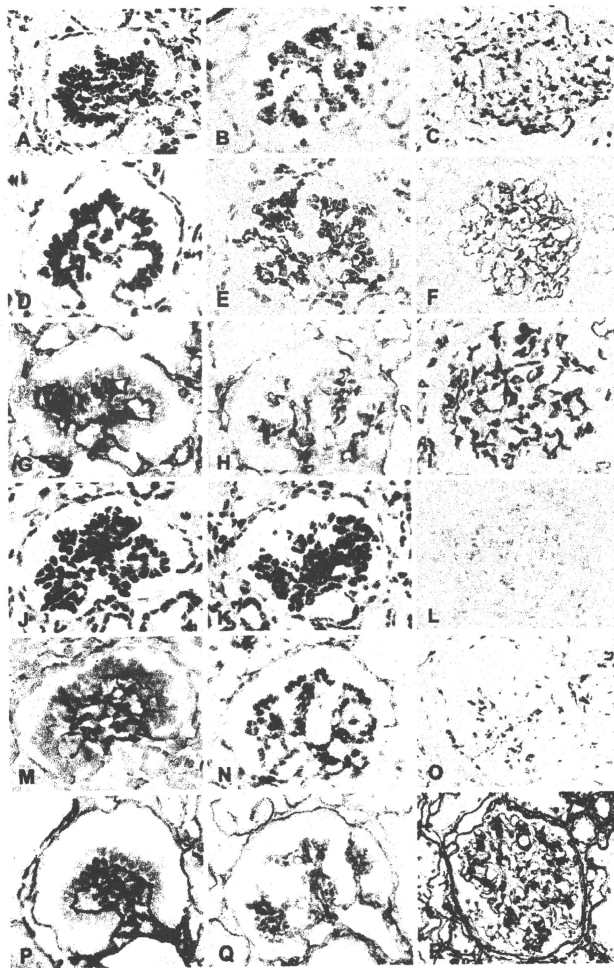
− 203 −
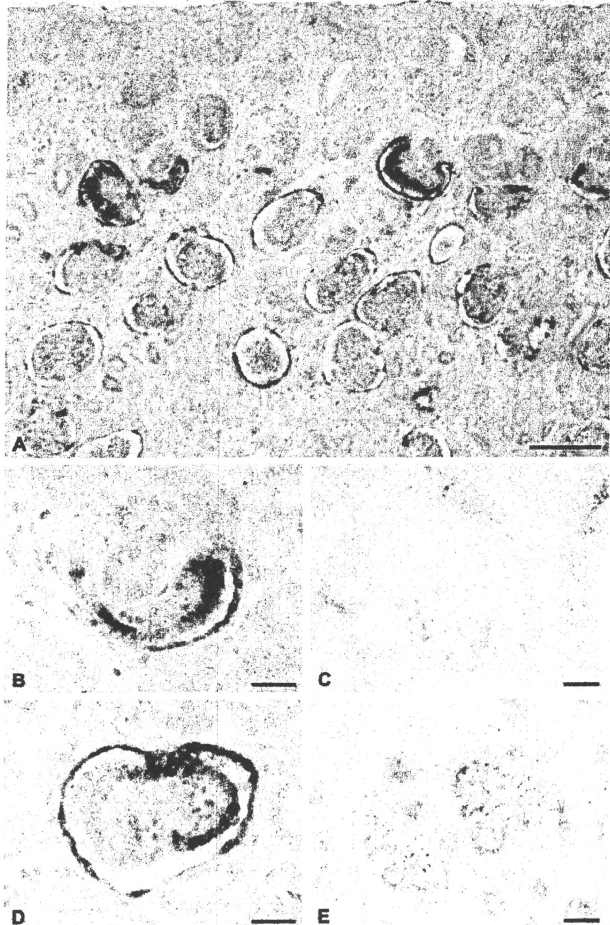
Fig. 4. Protein expression of CTGF (rabbit anti-CEADLEENIKK; *A*, *B*, and *C*), synaptopodin (*D*, *E*, and *F*), CD31 (*G*, *H*, and *I*), α-smooth muscle actin (SMA) (*J*, *K*, and *L*), fibronectin EDA (*M*, *N*, and *O*), and type IV collagen (*P*, *Q*, and *R*) in human glomeruli at the capillary loop stage (*A*, *D*, *G*, *J*, *M*, and *P*), the maturing stage (*B*, *E*, *H*, *K*, *N*, and *Q*), and at the adult stage (*C*, *F*, *I*, *L*, *O*, and *R*) detected by immunostaining with hematoxylin counterstain. Original magnifications: ×400 (*A*, *D*, *G*, *J*, *M*, *P*), ×250 (*B*, *E*, *H*, *K*, *N*, *Q*), ×100 (*C*, *F*, *I*, *L*, *O*, *R*). *A*: at the capillary loop stage, CTGF is expressed in the basal portion of the podocytes and in a mixed cell cluster at the root of the glomerulus. *B*: in maturing glomeruli, CTGF protein expression shows a more extended distribution, as podocytes and mesangial cells have migrated to the periphery. *C*: in the normal adult glomerulus, CTGF protein is mainly expressed by podocytes. Fibronectin-EDA is expressed from the capillary loop stage to the maturing glomerulus stage in association with presence of α-SMA-positive cells in the mesangial area.

mixed-cell cluster at the root of the glomerulus (Figs. 3*E* and 4*A*). Synaptopodin staining was restricted to the basal part of the GVECs (Fig. 4*D*), which display a columnar shape and have not yet formed foot processes in this stage. CD31 positive endothelial cells were present with α-SMA-positive mesenchymal cells in small groups at the root of the immature glomerulus (Fig. 4, *G* and *J*). In addition, CD31-positive endothelial cells could be found in a layer in juxtaposition to the GVEC, thereby forming immature glomerular capillaries; CD31 staining of these endothelial cells was restricted to their luminary aspect (Fig. 4*G*). Glomerular EDA-FN was abundant in this stage of nephrogenesis in a similar distribution pattern as observed for type IV collagen, being localized at the basal portion of the podocytes, and in between the clustered endothelial and mesenchymal cells, as well as along the Bowman's capsule (Fig. 4, *M* and *P*).

In the maturing glomerulus stage, the number of endothelial cells and mesangial precursor cells is strongly increased, and the glomerular capillary network is formed. CTGF was detected in a scattered pattern along the capillary wall and in the

— 204 —

Fig. 5. Double immunofluorescence immunostaining for protein expression of CTGF (rabbit anti-CEADLEENIKK; red) and synaptopodin, α-SMA, or CD31 (all green) during human glomerulogenesis analyzed by confocal laser scanning microscopy; double-positive areas are depicted in yellow. Original magnifications: ×400 (capillary loop stage), ×250 (maturing stage), ×100 (adult stage). In the capillary loop stages, CTGF is expressed by synaptopodin-positive podocytes, α-SMA-positive cells, and CD31-positive endothelial cells. In maturing glomerulus stages, CTGF is detected in podocytes and α-SMA-positive mesangial cells, but not in CD31-positive endothelial cells. In normal adult glomeruli, CTGF expression is restricted to the podocytes; the single red staining indicates CTGF-positive podocyte cell bodies, apical from the synaptopodin-positive terminal foot processes.
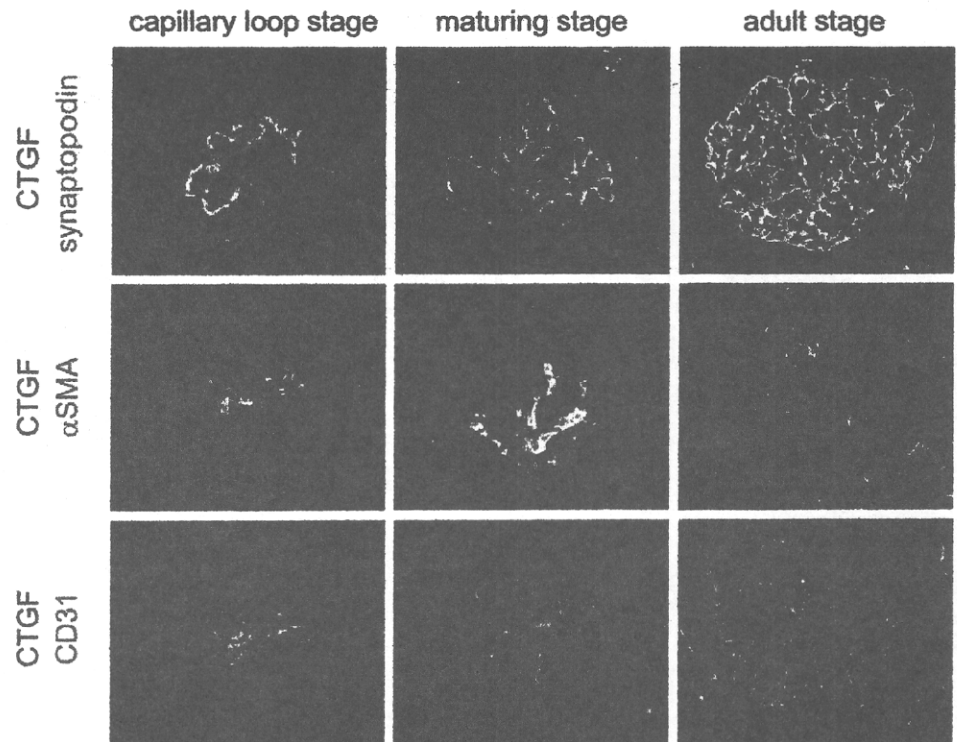
mesangial area, where α-SMA staining was positive (Fig. 4, B and K). Synaptopodin-positive GVEC and CD31-positive endothelial cells were found in the periphery of the glomerular tuft (Fig. 4, E and H). EDA-FN and type IV collagen were present in the mesangial area and type IV collagen also in Bowman's capsule (Figs. 4, N and Q).

In the adult glomerulus, CTGF is mainly expressed by podocytes (Fig. 4C). Synaptopodin is localized in the foot processes of podocytes along the glomerular basement membrane (Fig. 4F). In the adult kidney, mesangial CTGF expression decreased in association with diminished expression of α-SMA and EDA-FN (Fig. 4, C, L, and O), whereas type IV collagen is abundantly present in the glomerular basement membrane (Fig. 4R).

Double immunostaining for CTGF and synaptopodin, α-SMA, or CD31 was performed to examine the localization of CTGF in detail by confocal laser scanning microscopy (Fig. 5). In the capillary loop stages, CTGF protein was observed in the basal part of the podocytes, in α-SMA-positive cells, and in CD31-positive endothelial cells. In the maturing glomerulus stages, CTGF protein was detected in podocytes and α-SMA-positive mesangial cells, but not in CD31-positive endothelial cells. In the normal adult glomeruli, CTGF protein expression was confined to the podocytes. In particular, CTGF single staining can be observed in the cell body of the podocytes, apical of the synaptopodin-positive area that is adjacent to the basolateral membrane of the podocyte foot processes (Fig. 5). These distribution patterns could be confirmed for podocytes also by conventional light microscopy using double immunostaining (Supplemental Fig. S4).

Expression of TGF-β1, TGF-β2, and TGF-β3 proteins in human fetal and adult kidney. To investigate the possible relation between expression of CTGF and that of the TGF-β isoforms during glomerulogenesis, sections of human fetal and adult kidneys were stained for these proteins.

In the capillary loop stage, staining for TGF-β1, TGF-β2, and TGF-β3 was present in the basal portion of the GVEC (Fig. 6), similar to that for CTGF (Figs. 3E, 4A, 5, and 6). TGF-β1 and CTGF protein were also weakly detected in the mixed cluster of mesangial and endothelial cell precursors in the developing glomerular tuft (Figs. 5 and 6). TGF-β2 showed weak staining in the capillary loop stage (Fig. 6).

In the maturing glomerulus stage, the expression patterns of all TGF-β isoforms were similar to that of CTGF (Fig. 6), which was expressed by differentiating podocytes and α-SMA-positive mesangial cells (Figs. 4B and 5).

In the normal adult glomerulus, TGF-β2 and TGF-β3 (Fig. 6), as well as CTGF (Figs. 4C, 5, and 6), were mainly expressed by podocytes (Fig. 6). In contrast, TGF-β1 was not or only weakly detected (Fig. 6). CTGF was faintly detected in distal tubules and/or connecting segments in one-third of adult kidney tissues. TGF-β1, -β2, and -β3 were variably detected in tubular epithelial cells in adult kidneys. TGF-β1 staining was localized at the apical sites of a subset of tubular epithelial cells.

Expression of CTGF and TGF-β1, -β2, and -β3 in human glomerulopathies. In the noninflammatory glomerular diseases examined, i.e., minimal change nephropathy (Fig. 7) and idiopathic membranous glomerulopathy (MGP) (not shown), CTGF mRNA and protein expression were not upregulated in the mesangial area. However, in ~50% of biopsies of minimal change nephrotic syndrome (MCNS) (5/11) and MGP without glomerulosclerosis (6/11), CTGF expression was increased in podocytes and was detected in a continuous pattern along the glomerular capillary wall (Fig. 8A; rabbit anti-CEADLEENIKK). In the remaining subjects of MCNS and MGP, no upregulation of CTGF
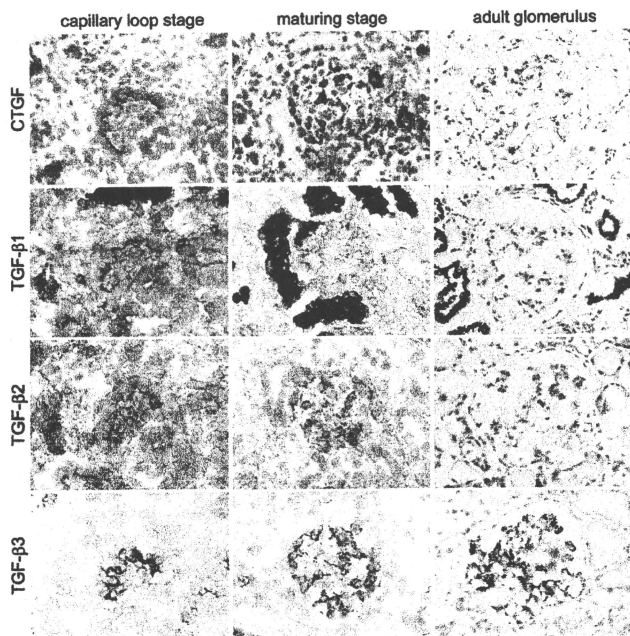
Fig. 6. Protein expression of CTGF (rabbit anti-CEADLEENIKK), TGF-β$_1$, TGF-β$_2$, and TGF-β$_3$ during human glomerulogenesis detected by immunostaining with hematoxylin counterstain. Original magnifications: ×400 (capillary loop stage), ×250 (maturing stage), ×100 (adult stage). In the capillary loop stages, CTGF protein is expressed in the basal portion of the podocytes and in a mixed-cell cluster within the glomerular tuft. TGF-β$_1$, TGF-β$_2$, and TGF-β$_3$ are detected in the basal portion of the podocytes. Also TGF-β$_1$ is weakly detected in the mixed-cell cluster. In the maturing glomerular stages, the expression pattern of each TGF-β isoform is similar to that of CTGF. In the normal adult glomerulus, TGF-β$_2$ and TGF-β$_3$, as well as CTGF, are mainly expressed by podocytes. TGF-β$_1$ is only detected in the tubules.

was observed in epithelial regions compared with control renal tissue samples. In MCNS and MGP, staining for the TGF-β isoforms was not different from that in normal control kidneys.

CTGF expression was increased in inflammatory glomerular and tubulo-interstitial lesions, associated with cell proliferation and matrix accumulation. Increased CTGF mRNA expression was predominantly observed in podocytes (Fig. 7). Concomitantly, CTGF protein was also strongly detected in podocytes, both with FG-3145 (Fig. 7) and with rabbit anti-CEADLEENIKK (Fig. 8, A and B). In addition, CTGF protein was detected in the mesangial proliferative lesions in IgA NP (Fig. 8A), diabetic nephropathy (Fig. 8B), and lupus nephritis (WHO class IV, Fig. 8B) with rabbit anti-CEADLEENIKK (Fig. 8), but not with FG-3145 (Fig. 7).

Although CTGF was abundant in these proliferative lesions, it was not detected in adjacent obsolescent glomeruli and completely sclerotic glomerular lesions, such as in diabetic nodular lesions (not shown). CTGF was strongly expressed in tubulo-interstitial fibrotic areas (not shown).

In case of mild mesangial proliferation, increased presence of CTGF, TGF-β$_2$ and TGF-β$_3$, but not of TGF-β$_1$, was observed (mild proliferative IgA NP, Fig. 8A). In contrast, expression of CTGF and of all isoforms of TGF-β was strongly increased in severe proliferative lesions (crescentic glomerulonephritis, Figs. 7 and 8B). In all kidney diseases examined, TGF-β$_1$ expression was increased to a larger extent in tubulo-

interstitial fibrotic areas than in glomerular lesions (not shown).

By semiquantitative analysis, the "mesangial CTGF protein expression score", as determined by immunostaining with rabbit anti-CEADLEENIKK, was significantly higher in IgA NP and diabetic glomerulosclerosis than in nonproliferative renal diseases and control kidneys (Fig. 9). In addition, in mesangial lesions of IgA NP, CTGF expression was much higher when proteinuria exceeded values of 1 g/day than in those of IgA NP patients with proteinuria of <1 g/day.

DISCUSSION

The expression of CTGF is increased in fibrotic disorders in a large variety of organs in association with simultaneous overexpression of TGF-β. Indeed, the well-known profibrotic factor TGF-β is the most potent inducer of CTGF expression to date. The presence of extracellular CTGF is required for effectuation of several of the profibrotic effects of TGF-β, as indicated by blocking studies in experimental models, both in vivo and in vitro (9, 20, 34, 67). Moreover, CTGF and TGF-β synergistically stimulate development of fibrosis upon administration in vivo (34). In this respect, two alternative, but not exclusive, hypotheses on the action of CTGF have emerged. First, CTGF may modulate signaling upon binding to various cell surface receptors (15, 33, 52, 59, 64). Second, CTGF may

PAS   CTGF mRNA   CTGF protein
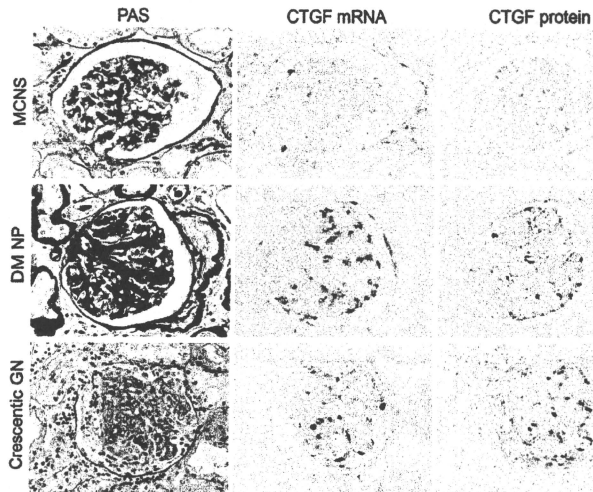

Fig. 7. Periodic acid Schiff (PAS) staining and expression of CTGF mRNA (in situ hybridization, blue signal; no counterstain) and CTGF protein (immunostaining using FG-3145, brown signal; methyl-green counterstain) in renal biopsy specimens from patients with minimal change nephritic syndrome (MCNS), diabetic glomerulosclerosis, and crescentic glomerulonephritis (GN). CTGF expression is increased mainly in podocytes in both mesangial and extracapillary proliferative lesions. Original magnifications: ×400. DM, diabetic mellitus; NP, nephropathy.

directly bind TGF-β and subsequently enhance binding of TGF-β to its signaling receptor (1). Here, we have confirmed coexpression of CTGF and TGF-β isoforms in several types of glomerular injury and have, in addition, shown a similar orchestrated coexpression during nephron development. We demonstrated that sustained expression of CTGF mRNA and CTGF protein is present in the renal glomeruli from the S-shaped stage onward, and that the glomerular CTGF expression is in all stages associated with colocalized expression of at least one of the TGF-β family members. To our knowledge, this is the first time that such simultaneous and colocalized expression of CTGF and TGF-β is described in the absence of development of fibrosis.

Interaction of the multidomain CTGF with various ligands may affect its detection, possibly explaining the different subcellular staining patterns of the antibodies directed against either domain 2 (FG-3019, FG-3145) or domain 3–4 (rabbit anti-CEADLEENIKK). Physiological CTGF cleavage products may occur at various sites as well. CTGF protein was abundant in a punctate pattern in a subset of tubular epithelial cells in newborn rat kidneys, as detected using the antidomain 2, but not with the antidomain 3–4 antibodies. Since CTGF mRNA was hardly expressed in these cells, this observation suggests that CTGF may be endocytosed by tubular epithelial cells. Indeed, CTGF can bind and modulate signaling via LDL receptor-related protein scavenging receptors (33, 52) and is degraded in endosomes (16). The in vivo dynamics of CTGF turnover and processing require more investigation.

The overall expression patterns of CTGF during glomerulogenesis in rat and humans correspond with each other. Further analysis revealed that, in the capillary loop stage, CTGF mRNA and protein are predominantly expressed by synaptopodin-positive GVECs; at this stage, CTGF protein is also present on α-SMA-positive precursors of mesangial cells and CD31-

positive precursors of glomerular endothelial cells. Paracrine effects of podocyte-derived CTGF on precursors of the other glomerular cell types may be envisaged, as has been demonstrated for VEGF-A (19). In maturation, CTGF protein expression became restricted to podocytes in adult glomeruli. Expression of TGF-β1 was high in the capillary loop stage and subsequently diminished to undetectable levels. Inversely, TGF-β2 was weakly detected in the capillary loop stage and was clearly present in fully matured podocytes at the adult age. Expression of TGF-β3 was observed in podocytes at all glomerular stages.

Previously, our laboratory showed that TGF-β1, TGF-β2, and TGF-β3 may all induce CTGF gene transcription in mesangial and podocyte cell lines to a similar extent (24). All TGF-β isoforms are capable to stimulate production of extracellular matrix proteins in renal fibroblasts, tubular epithelial cells, and mesangial cells in vitro (68). Upon forming a complex with TGF-β receptor type I and type II, each of the three TGF-β isoforms may cause activation of the Smad2 and Smad3 signaling intermediates, that subsequently bind Smad4 and translocate to the nucleus as a transcription activating complex (55). Induction of CTGF gene transcription by TGF-β in fibroblasts and mesangial cells in vitro involves signaling through Smad, MAP kinase, PKC, and Ets1 dependent pathways (8, 38). Expression of Smad2 and Smad3, the phosphorylated active pSmad2, and the common mediator Smad4 is widespread in early stages of nephron development, decreases with maturation, but remains present in podocytes in adult kidneys (4). Interestingly, Wu and colleagues (63) described an increased production of TGF-β2 and its requirement to induce cell-cycle arrest and differentiation in a model of podocyte maturation in vitro; the levels of TGF-β1 did not change. In contrast, addition of higher concentrations of either TGF-β1 or TGF-β2 induced apoptosis of podocytes in this model (63).
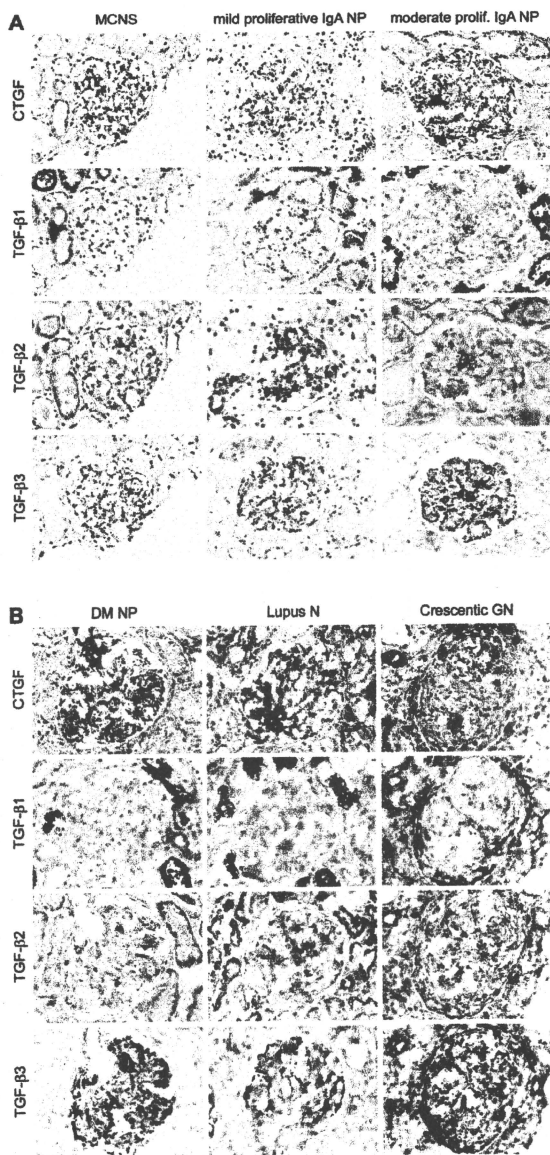
Fig. 8. Protein expression of CTGF (rabbit anti-CEADLEENIKK), TGF-β₁, TGF-β₂, and TGF-β₃ in MCNS, mild proliferative IgA NP, and moderate proliferative IgA NP (A), DM NP, World Health Organization class IV lupus nephritis (N), and crescentic GN (B). TGF-β₁ is not detected in glomeruli of MCNS and mild proliferative IgA NP. Expression of CTGF and of all isoforms of TGF-β is increased in the severe proliferative glomerular lesions. Immunostaining is with hematoxylin counterstain. Original magnifications: ×400.
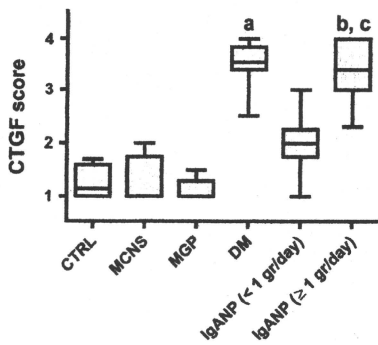
— 208 —

Fig. 9. Semiquantitative analysis of glomerular mesangial expression of CTGF protein in renal disorders, with or without mesangial expansion. Kidneys were examined of control subjects (CTRL; $n = 6$), MCNS ($n = 9$), idiopathic membranous glomerulopathy (MGP; $n = 11$), DM NP ($n = 10$), and IgA NP [subgrouped in patients with proteinuria <1 g/day ($n = 10$) and patients with proteinuria of at least 1 g/day ($n = 24$)]. Results are expressed as box-and-whisker plots; the boxes comprise the 25th and 75th percentiles and show the median values, the extremes are represented by the whiskers. Differences between groups were evaluated by the nonparametric Kruskal-Wallis and Dunn's multiple-comparison tests. [a] DM compared with CTRL, $P < 0.01$; DM compared with MCNS or MGP, $P < 0.001$. [b] IgA NP (≥1 g/day) compared with CTRL, MCNS, or MGP, all $P < 0.001$. [c] IgA NP (≥1 g/day) compared with IgA NP (<1 g/day), $P < 0.05$.

Recent studies by Sims-Lucas and colleagues (56) using TGF-β_2 homozygous and heterozygous mutant mice also suggest that a critical and possible narrow range of TGF-β_2 concentrations is required for normal branching morphogenesis and nephrogenesis.

Our data, indicating the continuous presence of TGF-β_2 in fully differentiated podocytes under normal conditions in vivo, support the in vitro observations by Wu and colleagues (63). These observations suggest that the TGF-β-Smad signaling pathway is active in podocytes at all stages of development and may be involved in the apparently constitutive CTGF expression in these cells. Homozygous CTGF knockout mice die shortly after birth because of respiratory failure due to defective endochondral ossification and associated skeletal abnormalities (25, 26). To what extent CTGF contributes to maintaining normal glomerular form and function is, therefore, not clear at present.

The early stages of glomerular development, in which coexpression of TGF-β_1 and CTGF was observed, are characterized by processes like cell migration, proliferation, and matrix production that are also common in proliferative glomerulopathies and that are known to be induced by TGF-β_1 and CTGF in various cell types in vitro (8, 9, 21, 29, 37, 47). In agreement with earlier reports (3, 39), α-SMA expression was common in the mesangial area in the capillary loop stage. In addition, strong expression of the EDA-containing fibronectin splice variant was present. Interestingly, the presence of the EDA-FN domain is crucial for myofibroblastic phenotype induction by TGF-β_1 (53), a common phenomenon upon renal tissue injury. CTGF promotes migration of mesangial cells in an in vitro model for wound repair (9). We observed that transformation

of mesangial cells into α-SMA expressing myofibroblast-like cells was induced by TGF-β_1, but not affected by CTGF. However, CTGF was shown to be able to induce synthesis of fibronectin, type I collagen, and type IV collagen by mesangial cells (9). In an experimental model of tubulointerstitial nephritis, antisense blocking of CTGF expression resulted in reduced expression of EDA-FN (66).

The results of the present study support the concept that overexpression of CTGF and TGF-β_1 contributes to development of renal fibrosis in adults. CTGF mRNA is upregulated in proliferative lesions of human and experimental glomerulonephritis, in particular in extracapillary proliferative lesions, confirming previous reports (23, 24). Here, we extend these observations by detailing CTGF expression at the protein level. We further explored the relation between glomerular CTGF and TGF-β protein expression in several types of human glomerulopathies. The mesangial CTGF expression score was significantly increased in diabetic glomerulosclerosis and in IgA NP, in particular, in subjects with high proteinuria. In these lesions, CTGF mRNA is predominantly expressed by podocytes, which are, therefore, probably the main source of full-length CTGF protein. In accordance, both NH$_2$-terminal and COOH-terminal domains of CTGF were detected in podocytes. Interestingly, predominantly COOH-terminal CTGF was detected in the mesangial area, warranting further investigation of possible CTGF cleavage and differential availability of CTGF fragments in these glomerulopathies. In nonproliferative glomerular diseases, such as minimal change nephropathy and MGP, the mesangial CTGF expression score was not different from that in control kidneys. Yokoi and colleagues (65) recently demonstrated in podocyte-specific CTGF-transgenic mice that CTGF overexpression per se does not cause glomerulopathy in otherwise normal mice. Importantly, streptozotocin-induced diabetes resulted in more severe diabetic nephropathy in the CTGF-transgenic mice than in their wild-type littermates (65). SMAD3-dependent signaling is involved in development of diabetic glomerulosclerosis (60), in line with the widely appreciated role of TGF-β in renal fibrosis (7, 10). Accordingly, high expression of all TGF-β isoforms was present in severe proliferative lesions, including diabetic glomerulosclerosis. TGF-β_1 expression was less in mild mesangial proliferative lesions and in nonproliferative glomerulopathies. More than one-half of the subjects with MCNS or MGP showed no expression of TGF-β_1 in the glomerulus, whereas relatively strong expression of TGF-β_2 and TGF-β_3 was present in podocytes. These findings are in agreement with those from several experimental models in which also all TGF-β isoforms were present in only the most severe cases of glomerulonephritis (24, 54, 62).

In summary, our findings suggest that coordinated expression of TGF-β isoforms and of CTGF may be involved in normal glomerulogenesis and possibly in maintenance of glomerular structure and function at adult age. Prolonged overexpression of TGF-β_1 and CTGF is associated with development of severe glomerulonephritis and glomerulosclerosis.

Gerritsen (Dept. of Internal Medicine, University Medical Centre Utrecht, Utrecht, The Netherlands) for performing ELISA to CTGF. Present address of J. J. Weening: TerGooi Hospitals, Blaricum, The Netherlands.

REFERENCES

1. **Abreu JG, Ketpura NI, Reversade B, De Robertis EM.** Connective-tissue growth factor (CTGF) modulates cell signalling by BMP and TGF-beta. *Nat Cell Biol* 4: 599–604, 2002.
2. **Alpers CE, Hudkins KL, Gown AM, Johnson RJ.** Enhanced expression of "muscle-specific" actin in glomerulonephritis. *Kidney Int* 41: 1134–1142, 1992.
3. **Alpers CE, Seifert RA, Hudkins KL, Johnson RJ, Bowen-Pope DF.** Developmental patterns of PDGF B-chain, PDGF-receptor, and alpha-actin expression in human glomerulogenesis. *Kidney Int* 42: 390–399, 1992.
4. **Banas MC, Parks WT, Hudkins KL, Banas B, Holdren M, Iyoda M, Wietecha TA, Kowalewska J, Liu G, Alpers CE.** Localization of TGF-beta signaling intermediates Smad2, 3, 4, and 7 in developing and mature human and mouse kidney. *J Histochem Cytochem* 55: 275–285, 2007.
5. **Barisoni L, Kriz W, Mundel P, D'Agati V.** The dysregulated podocyte phenotype: a novel concept in the pathogenesis of collapsing idiopathic focal segmental glomerulosclerosis and HIV-associated nephropathy. *J Am Soc Nephrol* 10: 51–61, 1999.
6. **Barisoni L, Mokrzycki M, Sablay L, Nagata M, Yamase H, Mundel P.** Podocyte cell cycle regulation and proliferation in collapsing glomerulopathies. *Kidney Int* 58: 137–143, 2000.
7. **Blobe GC, Schiemann WP, Lodish HF.** Role of transforming growth factor beta in human disease. *N Engl J Med* 342: 1350–1358, 2000.
8. **Blom IE, Goldschmeding R, Leask A.** Gene regulation of connective tissue growth factor: new targets for antifibrotic therapy? *Matrix Biol* 21: 473–482, 2002.
9. **Blom IE, van Dijk AJ, Wieten L, Duran K, Ito Y, Kleij L, deNichilo M, Rabelink TJ, Weening JJ, Aten J, Goldschmeding R.** In vitro evidence for differential involvement of CTGF, TGFbeta, and PDGF-BB in mesangial response to injury. *Nephrol Dial Transplant* 16: 1139–1148, 2001.
10. **Border WA, Noble NA.** Transforming growth factor beta in tissue fibrosis. *N Engl J Med* 331: 1286–1292, 1994.
11. **Bork P.** The modular architecture of a new family of growth regulators related to connective tissue growth factor. *FEBS Lett* 327: 125–130, 1993.
12. **Borsi L, Carnemolla B, Castellani P, Rosellini C, Vecchio D, Allemanni G, Chang SE, Taylor-Papadimitriou J, Pande H, Zardi L.** Monoclonal antibodies in the analysis of fibronectin isoforms generated by alternative splicing of mRNA precursors in normal and transformed human cells. *J Cell Biol* 104: 595–600, 1987.
13. **Brigstock DR.** The connective tissue growth factor/cysteine-rich 61/nephroblastoma overexpressed (CCN) family. *Endocr Rev* 20: 189–206, 1999.
14. **Brigstock DR, Goldschmeding R, Katsube KI, Lam SC, Lau LF, Lyons K, Naus C, Perbal B, Riser B, Takigawa M, Yeger H.** Proposal for a unified CCN nomenclature. *Mol Pathol* 56: 127–128, 2003.
15. **Chen CC, Chen N, Lau LF.** The angiogenic factors Cyr61 and connective tissue growth factor induce adhesive signaling in primary human skin fibroblasts. *J Biol Chem* 276: 10443–10452, 2001.
16. **Chen Y, Segarini P, Raoufi F, Bradham D, Leask A.** Connective tissue growth factor is secreted through the Golgi and is degraded in the endosome. *Exp Cell Res* 271: 109–117, 2001.
17. **Clark AT, Young RJ, Bertram JF.** In vitro studies on the roles of transforming growth factor-beta 1 in rat metanephric development. *Kidney Int* 59: 1641–1653, 2001.
18. **Costantini F.** Renal branching morphogenesis: concepts, questions, and recent advances. *Differentiation* 74: 402–421, 2006.
19. **Eremina V, Cui S, Gerber H, Ferrara N, Haigh J, Nagy A, Ema M, Rossant J, Jothy S, Miner JH, Quaggin SE.** Vascular endothelial growth factor a signaling in the podocyte-endothelial compartment is required for mesangial cell migration and survival. *J Am Soc Nephrol* 17: 724–735, 2006.
20. **Frazier K, Williams S, Kothapalli D, Klapper H, Grotendorst GR.** Stimulation of fibroblast cell growth, matrix production, and granulation tissue formation by connective tissue growth factor. *J Invest Dermatol* 107: 404–411, 1996.
21. **Grotendorst GR, Lau LF, Perbal B.** CCN proteins are distinct from and should not be considered members of the insulin-like growth factor-binding protein superfamily. *Endocrinology* 141: 2254–2256, 2000.
22. **Igarashi A, Nashiro K, Kikuchi K, Sato S, Ihn H, Fujimoto M, Grotendorst GR, Takehara K.** Connective tissue growth factor gene expression in tissue sections from localized scleroderma, keloid, and other fibrotic skin disorders. *J Invest Dermatol* 106: 729–733, 1996.
23. **Ito Y, Aten J, Bende RJ, Oemar BS, Rabelink TJ, Weening JJ, Goldschmeding R.** Expression of connective tissue growth factor in human renal fibrosis. *Kidney Int* 53: 853–861, 1998.
24. **Ito Y, Goldschmeding R, Bende R, Claessen N, Chand M, Kleij L, Rabelink T, Weening J, Aten J.** Kinetics of connective tissue growth factor expression during experimental proliferative glomerulonephritis. *J Am Soc Nephrol* 12: 472–484, 2001.
25. **Ivkovic S, Yoon BS, Popoff SN, Safadi FF, Libuda DE, Stephenson RC, Daluiski A, Lyons KM.** Connective tissue growth factor coordinates chondrogenesis and angiogenesis during skeletal development. *Development* 130: 2779–2791, 2003.
26. **Katsube K, Sakamoto K, Tamamura Y, Yamaguchi A.** Role of CCN, a vertebrate specific gene family, in development. *Dev Growth Differ* 51: 55–67, 2009.
27. **Kireeva ML, Latinkic BV, Kolesnikova TV, Chen CC, Yang GP, Abler AS, Lau LF.** Cyr61 and Fisp12 are both ECM-associated signaling molecules: activities, metabolism, and localization during development. *Exp Cell Res* 233: 63–77, 1997.
28. **Kitamurti U, Chen Y, Michael A, Kim Y, Fan WW, Wieslander J, Brunmark C, Rondeau E, Sraer JD, Delarue F, Tsilibary EC.** Integrin-mediated interactions between primary/T-sv40 immortalized human glomerular epithelial cells and type IV collagen. *Lab Invest* 74: 650–657, 1996.
29. **Lau LF, Lam SC.** The CCN family of angiogenic regulators: the integrin connection. *Exp Cell Res* 248: 44–57, 1999.
30. **Leask A, Abraham DJ.** TGF-beta signaling and the fibrotic response. *FASEB J* 18: 816–827, 2004.
31. **Letterio JJ, Geiser AG, Kulkarni AB, Roche NS, Sporn MB, Roberts AB.** Maternal rescue of transforming growth factor-beta 1 null mice. *Science* 264: 1936–1938, 1994.
32. **Liu A, Dardik A, Ballermann BJ.** Neutralizing TGF-beta1 antibody infusion in neonatal rat delays in vivo glomerular capillary formation 1. *Kidney Int* 56: 1334–1348, 1999.
33. **Mercurio S, Latinkic B, Itasaki N, Krumlauf R, Smith JC.** Connective tissue growth factor modulates WNT signalling and interacts with the WNT receptor complex. *Development* 131: 2137–2147, 2004.
34. **Mori T, Kawara S, Shinozaki M, Hayashi N, Kakinuma T, Igarashi A, Takigawa M, Nakanishi T, Takehara K.** Role and interaction of connective tissue growth factor with transforming growth factor-beta in persistent fibrosis: a mouse fibrosis model. *J Cell Physiol* 181: 153–159, 1999.
35. **Mundel P, Reiser J, Zuniga Mejia Borja A, Pavenstadt H, Davidson GR, Kriz W, Zeller R.** Rearrangements of the cytoskeleton and cell contacts induce process formation during differentiation of conditionally immortalized mouse podocyte cell lines. *Exp Cell Res* 236: 248–258, 1997.
36. **Munger JS, Harpel JG, Gleizes PE, Mazzieri R, Nunes I, Rifkin DB.** Latent transforming growth factor-beta: structural features and mechanisms of activation. *Kidney Int* 51: 1376–1382, 1997.
37. **Murphy M, Godson C, Cannon S, Kato S, Mackenzie HS, Martin F, Brady HR.** Suppression subtractive hybridization identifies high glucose levels as a stimulus for expression of connective tissue growth factor and other genes in human mesangial cells. *J Biol Chem* 274: 5830–5834, 1999.
38. **Nakerakanti SS, Kapanadze B, Yamasaki M, Markiewicz M, Trojanowska M.** Fli1 and Ets1 have distinct roles in connective tissue growth factor/CCN2 gene regulation and induction of the profibrotic gene program. *J Biol Chem* 281: 25259–25269, 2006.

39. Naruse K, Fujieda M, Miyazaki E, Hayashi Y, Toi M, Fukui T, Kuroda N, Hiroi M, Kurashige T, Enzan H. An immunohistochemical study of developing glomeruli in human fetal kidneys. *Kidney Int* 57: 1836–1846, 2000.

40. Oemar BS, Werner A, Garnier JM, Do DD, Godoy N, Nauck M, Marz W, Rupp J, Pech M, Luscher TF. Human connective tissue growth factor is expressed in advanced atherosclerotic lesions. *Circulation* 95: 831–839, 1997.

41. Oshima M, Oshima H, Taketo MM. TGF-beta receptor type II deficiency results in defects of yolk sac hematopoiesis and vasculogenesis. *Dev Biol* 179: 297–302, 1996.

42. Paradis V, Dargere D, Vidaud M, De Gouville AC, Huet S, Martinez V, Gauthier JM, Ba N, Sobesky R, Ratziu V, Bedossa P. Expression of connective tissue growth factor in experimental rat and human liver fibrosis. *Hepatology* 30: 968–976, 1999.

43. Pelton RW, Saxena B, Jones M, Moses HL, Gold LI. Immunohistochemical localization of TGF beta 1, TGF beta 2, and TGF beta 3 in the mouse embryo: expression patterns suggest multiple roles during embryonic development. *J Cell Biol* 115: 1091–1105, 1991.

44. Pennica D, Swanson TA, Welsh JW, Roy MA, Lawrence DA, Lee J, Brush J, Taneyhill LA, Deuel B, Lew M, Watanabe C, Cohen RL, Melhem MF, Finley GG, Quirke P, Goddard AD, Hillan KJ, Gurney AL, Botstein D, Levine AJ. WISP genes are members of the connective tissue growth factor family that are up-regulated in wnt-1-transformed cells and aberrantly expressed in human colon tumors. *Proc Natl Acad Sci U S A* 95: 14717–14722, 1998.

45. Plisov SY, Yoshino K, Dove LF, Higinbotham KG, Rubin JS, Perantoni AO. TGF beta 2, LIF and FGF2 cooperate to induce nephrogenesis. *Development* 128: 1045–1057, 2001.

46. Quigg RJ, Cybulsky AV, Jacobs JB, Salant DJ. Anti-Fx1A produces complement-dependent cytotoxicity of glomerular epithelial cells. *Kidney Int* 34: 43–52, 1988.

47. Riser BL, Denichilo M, Cortes P, Baker C, Grondin JM, Yee J, Narins RG. Regulation of connective tissue growth factor activity in cultured rat mesangial cells and its expression in experimental diabetic glomerulosclerosis. *J Am Soc Nephrol* 11: 25–38, 2000.

48. Rogers SA, Ryan G, Purchio AF, Hammerman MR. Metanephric transforming growth factor-beta 1 regulates nephrogenesis in vitro. *Am J Physiol Renal Fluid Electrolyte Physiol* 264: F996–F1002, 1993.

49. Sanford LP, Ormsby I, Gittenberger-de Groot AC, Sariola H, Friedman R, Boivin GP, Cardell EL, Doetschman T. TGFbeta2 knockout mice have multiple developmental defects that are non-overlapping with other TGFbeta knockout phenotypes. *Development* 124: 2659–2670, 1997.

50. Saxén L. *Organogenesis of the Kidney.* Cambridge, UK: Cambridge University Press, 1987, p. 173.

51. Schedl A, Hastie ND. Cross-talk in kidney development. *Curr Opin Genet Dev* 10: 543–549, 2000.

52. Segarini PR, Nesbitt JE, Li D, Hays LG, Yates JR 3rd, Carmichael DF. The low density lipoprotein receptor-related protein/alpha2-macroglobulin receptor is a receptor for connective tissue growth factor. *J Biol Chem* 276: 40659–40667, 2001.

53. Serini G, Bochaton-Piallat ML, Ropraz P, Geinoz A, Borsi L, Zardi L, Gabbiani G. The fibronectin domain ED-A is crucial for myofibroblastic

phenotype induction by transforming growth factor-beta1. *J Cell Biol* 142: 873–881, 1998.

54. Shankland SJ, Pippin J, Pichler RH, Gordon KL, Friedman S, Gold LI, Johnson RJ, Couser WG. Differential expression of transforming growth factor-beta isoforms and receptors in experimental membranous nephropathy. *Kidney Int* 50: 116–124, 1996.

55. Shi Y, Massague J. Mechanisms of TGF-beta signaling from cell membrane to the nucleus. *Cell* 113: 685–700, 2003.

56. Sims-Lucas S, Caruana G, Dowling J, Kett MM, Bertram JF. Augmented and accelerated nephrogenesis in TGF-beta2 heterozygous mutant mice. *Pediatr Res* 63: 607–612, 2008.

57. Surveyor GA, Brigstock DR. Immunohistochemical localization of connective tissue growth factor (CTGF) in the mouse embryo between days 7.5 and 14.5 of gestation. *Growth Factors* 17: 115–124, 1999.

58. Van Den Berg JG, Aten J, Chand MA, Claessen N, Dijkink L, Wijdenes J, Lakkis FG, Weening JJ. Interleukin-4 and interleukin-13 act on glomerular visceral epithelial cells. *J Am Soc Nephrol* 11: 413–422, 2000.

59. Wahab NA, Weston BS, Mason RM. Connective tissue growth factor CCN2 interacts with and activates the tyrosine kinase receptor TrkA. *J Am Soc Nephrol* 16: 340–351, 2005.

60. Wang A, Ziyadeh FN, Lee EY, Pyagay PE, Sung SH, Sheardown SA, Laping NJ, Chen S. Interference with TGF-beta signaling by Smad3-knockout in mice limits glomerulosclerosis without affecting albuminuria. *Am J Physiol Renal Physiol* 293: F1657–F1665, 2007.

61. Wang QJ, Frazier K, Zhang W, Nichols B, Folz AL, Usinger WR, Gray J, Krueger M, Molineaux CJ, Oliver NA, Bremer M, Lin AY. Effects of a monoclonal antibody to connective tissue growth factor (CTGF) in experimental organ fibrosis (Abstract). *J Am Soc Nephrol* 13: 315A, 2002.

62. Wilson HM, Minto AW, Brown PA, Erwig LP, Rees AJ. Transforming growth factor-beta isoforms and glomerular injury in nephrotoxic nephritis. *Kidney Int* 57: 2434–2444, 2000.

63. Wu DT, Bitzer M, Ju W, Mundel P, Bottinger EP. TGF-beta concentration specifies differential signaling profiles of growth arrest/differentiation and apoptosis in podocytes. *J Am Soc Nephrol* 16: 3211–3221, 2005.

64. Yang M, Huang H, Li J, Li D, Wang H. Tyrosine phosphorylation of the LDL receptor-related protein (LRP) and activation of the ERK pathway are required for connective tissue growth factor to potentiate myofibroblast differentiation. *FASEB J* 18: 1920–1921, 2004.

65. Yokoi H, Mukoyama M, Mori K, Kasahara M, Suganami T, Sawai K, Yoshioka T, Saito Y, Ogawa Y, Kuwabara T, Sugawara A, Nakao K. Overexpression of connective tissue growth factor in podocytes worsens diabetic nephropathy in mice. *Kidney Int* 73: 446–455, 2008.

66. Yokoi H, Mukoyama M, Nagae T, Mori K, Suganami T, Sawai K, Yoshioka T, Koshikawa M, Nishida T, Takigawa M, Sugawara A, Nakao K. Reduction in connective tissue growth factor by antisense treatment ameliorates renal tubulointerstitial fibrosis. *J Am Soc Nephrol* 15: 1430–1440, 2004.

67. Yokoi H, Mukoyama M, Sugawara A, Mori K, Nagae T, Makino H, Suganami T, Yahata K, Fujinaga Y, Tanaka I, Nakao K. Role of connective tissue growth factor in fibronectin expression and tubulointerstitial fibrosis. *Am J Physiol Renal Physiol* 282: F933–F942, 2002.

68. Yu L, Border WA, Huang Y, Noble NA. TGF-beta isoforms in renal fibrogenesis. *Kidney Int* 64: 844–856, 2003.

Supplementary Figure 1

Protein-A affinity purified rabbit IgG anti-CEADLEENIKK binds the C-terminal half of CTGF (C-CTGF, containing domains 3 and 4) as well as full length CTGF (CTGF-W, consisting of domains 1 – 4) and does not bind to the N-terminal half of CTGF (N-CTGF, containing domains 1 and 2). The CEADLEENIKK peptide is located in between domains 3 and 4.

Recombinant human CTGF-W, C-CTGF and N-CTGF were purified from cultures of CHO cells that had been transfected with the respective expression vectors. For ELISA, CTGF-W, C-CTGF and N-CTGF were each coated at 40 nM. Dilution series of rabbit anti-CEADLEENIKK were examined by ELISA for binding to CTGF and its fragments; shown are the results of rabbit anti-CEADLEENIKK assayed at 0.4 µg/ml.

Supplementary Figure 2

Expression of CTGF mRNA was detected by in situ hybridization using a DIG-labeled antisense riboprobe in formalin-fixed paraffin sections of rat kidneys at ages of 9 days (A), 1 day (C) and 5 days (E). Bound DIG is detected by immunostaining with alkaline phophatase-conjugated sheep anti-DIG antibody and nitroblue tetrazolium chloride and 5-bromo-4-chloro-3-indolylphosphate as substrate, yielding a blue precipitate. Incubation with the control DIG-labeled sense riboprobe on serial sections (B, D, E) does not yield any staining.

Following the ISH procedure, immunohistochemistry was performed for collagen type IV to provide a counterstain that does not interfere with the cellularly localized ISH signals. Binding of the rabbit anti-collagen type IV was detected with poly-HRP goat anti-rabbit IgG and 3,3'-diaminobenzidine and hydrogen peroxide as substrate, yielding a brown precipitate.

CTGF mRNA is detected in glomerular epithelial cells in capillary loop stage and maturing stage glomeruli. Bar sizes: 200 µm (A, B), 50 µm (C – F).
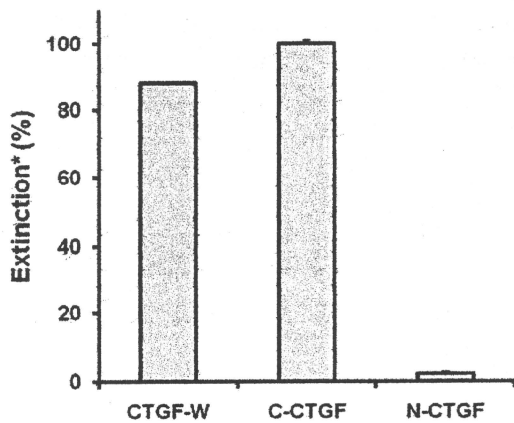
Supplementary Figure 3

Expression of CTGF protein in a rat kidney of 9 days old. Immunostaining using FG-3019 (specific for domain 2 in the N-terminal part of CTGF) on formalin-fixed paraffin section (A) and rabbit anti-CEADLEENIKK (specific for an epitope in the C-terminal part of CTGF, containing domains 3 and 4) on methanol-fixed cryostat section (B) shows presence of CTGF protein in capillary loop stage and in maturing stage glomeruli with both methods. Different staining patterns are apparent for the tubular compartment. FG-3019 binds a subset of tubular epithelial cells in a punctuate pattern (A), whereas rabbit anti-CEADLEENIKK binds to developing cortical collecting ducts in the medullary ray area (B). Replacement of the anti-CTGF antibodies with either normal human serum on paraffin sections (not

shown) or pre-immune normal rabbit serum on cryostat sections (C) did not yield any binding of the enzyme-conjugated secondary step reagents. Bar size: 100 μm.

Supplementary Figure 4

Double immunostaining for protein expression of CTGF (rabbit anti-CEADLEENIKK; red) and synaptopodin (blue) in a glomerular capillary loop stage (A) and in an adult glomerulus (B) of human kidneys. Original magnifications: x400.

At the capillary loop stage, CTGF is expressed by synaptopodin-positive epithelial cells and also by precursors of mesangial and glomerular endothelial cells. In the normal adult kidney glomerular CTGF expression is less abundant and restricted to podocytes. Supplementary Figure 4 confirms data presented in Figure 5, applying light microscopy of double-stained sections instead of confocal laser scanning fluorescence microscopy.

Supplementary Figure 1